Chinese Chemical Letters 35 (2024) 109791

Contents lists available at ScienceDirect

Chinese Chemical Letters

journal homepage: www.elsevier.com/locate/cclet

Benzothiadiazole-based water-soluble macrocycle: Synthesis, aggregation-induced emission and selective detection of spermine

Shuo Li[a,*], Qianfa Liu[a], Lijun Mao[a], Xin Zhang[a], Chunju Li[b,*], Da Ma[a,*]

[a] School of Pharmaceutical Engineering & Institute for Advanced Studies, Taizhou University, Taizhou 318000, China
[b] Tianjin Key Laboratory of Structure and Performance for Functional Molecules, College of Chemistry, Tianjin Normal University, Tianjin 300387, China

ARTICLE INFO

Article history:
Received 30 January 2024
Revised 8 March 2024
Accepted 18 March 2024
Available online 25 June 2024

Keywords:
Macrocycle
Water-soluble
Aggregation-induced emission
Biogenic amines
Host-guest interaction

ABSTRACT

Reported here is the synthesis of a new macrocycle bearing anionic carboxylate groups with water-soluble aggregation-induced emission (AIE). The water-soluble macrocycle without typical AIE luminogens is constructed based on the building block of benzothiadiazole. It exhibits a remarkable AIE effect. This water-soluble macrocycle can selectively bind different types of biogenic amines in aqueous media with the tightest binding towards spermine. The fluorescence enhancement induced by supramolecular encapsulation is used to detect spermine.

Organic luminescent macrocycles are powerful tools in supramolecular chemistry. The intrinsic optical features and interesting host-guest recognition capabilities of these macrocycles render them applications in biological sensing, photo-induced therapeutics and optoelectronics [1–7]. Although great progress has been achieved in synthesis and applications of organic luminescent macrocycles, most of them show poor solubility and weak host-guest interactions in water, which limits their use in biological sensing and other applications [8–18].

Currently, a promising strategy to construct water-soluble macrocycles with luminescence is incorporating π-conjugated chromophores (*e.g.*, pyrene, anthracene, azobenzene, perylene diimides and naphthalimide) into macrocyclic scaffolds [19–27]. Different from the traditional chromophores, aggregation-induced emission (AIE) molecules, an emerging class of concentration-dependent chromophores, have exhibited colossal potentials in sensing and imaging [28–35]. Almost all of the reported water-soluble AIE-active macrocycles have been constructed on the basis of the typical AIE luminogens tetraphenylethene (TPE), and are modified with cationic water-soluble groups, such as imidazolium salts, pyridinium salts and quaternary amine salts [36–38]. Water-soluble AIE macrocycles modified with anionic groups have been rarely reported. It is important to develop anionic group-bearing water-soluble AIE macrocycles to enhance the binding affinity and sensing capability.

In our previous work, we designed and synthesized a benzothiadiazole-based macrocycle (BT-OMe) with intense emission in the solid state [39]. This macrocycle did not contain orthodox AIE chromophores. The methoxy groups on the benzene skeleton make it easy to introduce water-soluble functional groups into the macrocyclic backbone. Here we introduce carboxylates as water soluble groups to this macrocycle, and develop an anionic group-bearing water-soluble AIE macrocycle. The twelve carboxylate anionic groups not only serve as solubilizing groups, but also enhance the supramolecular encapsulation via electrostatic interaction. The resulting water-soluble macrocycle demonstrates AIE effect, and selective binding towards biogenic amines in water, which renders it useful for the sensing of spermine.

The synthesis of water-soluble benzothiadiazole macrocycle (WBT) was outlined in Scheme 1a. The precursor BT-OMe was synthesized by a one-step condensation protocol [40]. Subsequently, methoxy groups were cleaved by BBr_3 to yield a per-hydroxylated cyclic trimer (BT-OH) in 83% yield. This compound reacted with ethyl bromoacetate under basic conditions (K_2CO_3) to prepare ethoxycarbonylmethoxy-substituted cyclic trimer (BT-COOEt, 70% yield). BT-COOEt was hydrolyzed in NaOH solution and then acidified with aqueous HCl to yield carboxylic acid-substituted cyclic trimer (BT-COOH, 82% yield) which is poorly soluble in water. Finally, treatment of BT-COOH with aqueous ammonia solution afforded the water-soluble AIE macrocycle (WBT) in 87% yield. All compounds were confirmed by ^1H and ^{13}C NMR spectroscopy and

* Corresponding authors.
E-mail addresses: shuoli@tzc.edu.cn (S. Li), cjli@shu.edu.cn (C. Li), dama@tzc.edu.cn (D. Ma).

https://doi.org/10.1016/j.cclet.2024.109791
1001-8417/

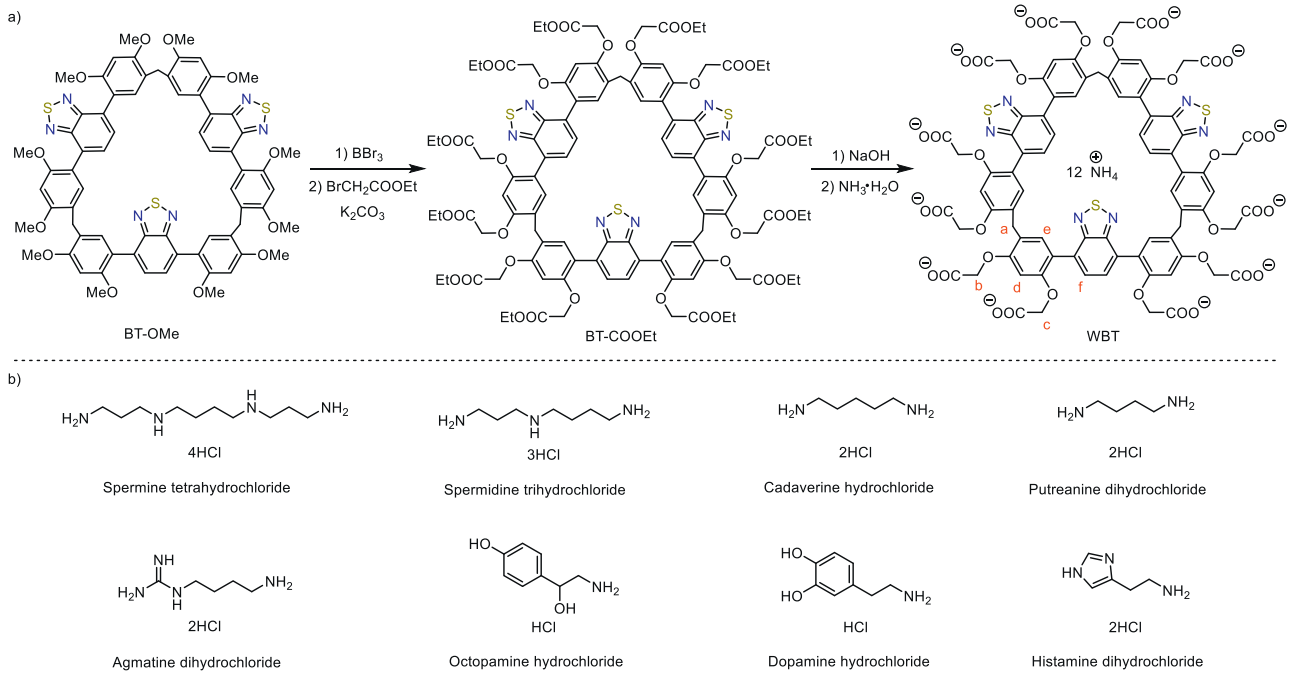

Scheme 1. (a) The synthetic route of water-soluble AIE macrocycle WBT. (b) Chemical structures of biogenic amines.

high-resolution mass spectra (Figs. S1-S12 in Supporting information).

The optical characteristics of water-soluble benzothiadiazole-based macrocycle WBT were first examined. The diffuse reflectance spectroscopy and fluorescence spectrum of WBT in the solid state are shown in Fig. 1a. WBT showed a broad absorption band and a maximum emission wavelength at 580 nm, which were attributed to intramolecular charge transfer (ICT) between benzothiadiazole acceptor and adjacent benzene ring donors. Its absolute fluorescence quantum yield in the solid state was measured to be 13.3% (Fig. S13 in Supporting information). Moreover, WBT exhibited concentration dependent fluorescence enhancement phenomenon. As shown in Fig. 1b and Fig. S14 (Supporting information), when the concentration of WBT increased from 1 μmol/L to 100 μmol/L, its emission intensity at 625 nm significantly enhanced. Then, photophysical behaviors of WBT in aggregated state were tested. As depicted in Figs. 1c and d, the fluorescent intensities of WBT gradually increased when dimethyl sulfoxide (DMSO) content in

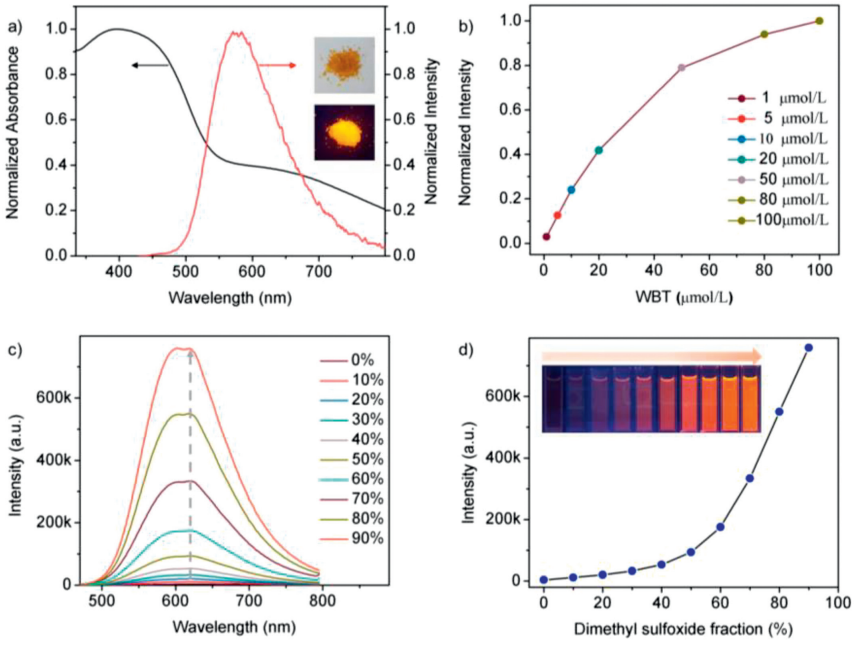

Fig. 1. (a) Normalized diffuse reflectance spectra (black line, left axis) and normalized fluorescence spectra (red line, right axis) of WBT in the solid state. Insets: photographs of WBT under natural light (top) or 365 nm illumination (bottom). (b) Fluorescence emission intensity of WBT at different concentrations. (c) Fluorescence spectra and (d) fluorescence intensity of WBT in water/DMSO mixtures with different fractions of DMSO (0–90%, v/v). λ_{ex} = 410 nm. Inset: photographs of WBT with different DMSO fractions taken under 365 UV illumination.

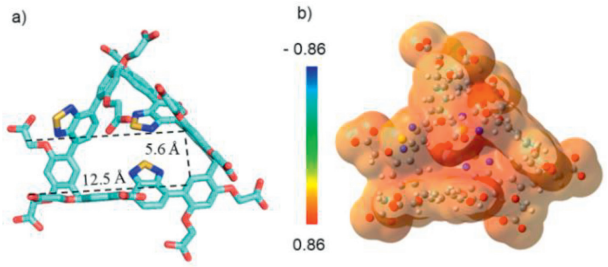

Fig. 2. (a) The optimized geometry of WBT. (b) Molecular surface electrostatic potential of WBT.

H_2O-DMSO mixture increase from 0 to 50%. As DMSO fractions (*f*w) further increases from 50% to 90%, the fluorescence intensity sharply increased. Meanwhile, the emission wavelengths showed a negligible redshift. These results indicated that the water-soluble macrocycle has the characteristics of AIE and concentration dependent luminescence enhancement. The reason for its AIE property is attributed to the rigid triangular structure of WBT [40].

The configuration of WBT were then optimized on the basis of density functional theory (DFT) at the B3LYP-D3/6-31G+(d,p) level. In the simulated structure (Fig. 2a), WBT formed a triangular structure where two benzothiadiazole units extend into the interior of the cavity. Although the macrocyclic cavity is occupied by benzothiadiazoles, three dimethoxyphenyl walls located at the same portal of macrocycle cavity formed a pseudo cavity like a tunnel with a size of 5.6 Å × 12.5 Å, which is spacious enough to be threaded by spermine. Therefore, the macrocycle still has enough space to accommodate guest molecules. Surface electrostatic potential map indicated that these dimethoxyphenyl walls and carboxylate side chains are relatively electron rich and should be able to interact with positively charged and electron-poor guests (Fig. 2b). Given that its shape, cavity size, as well as electron-rich sidewalls and side chains, WBT may be a suitable molecular container for aliphatic amines.

Biogenic amines (BAs) are a class of biomolecules produced by decarboxylation of free amino acids or by amination and transamination of aldehydes and ketones [40,41]. These amines can be found at high concentrations both in tumor cell and fermented food. Therefore, selective detection of biogenic amines is significant in cancer diagnosis and food safety. Subsequently, host-guest complexation of WBT towards different types of biogenic amines (Scheme 1b) was investigated, including aliphatic amines (*e.g.*, spermine, spermidine, agmatine, cadaverine, putrescine), aromatic amines (*e.g.*, octopamine, dopamine), and heterocyclic amine (*e.g.*, histamine).

The binding between WBT and spermine was first examined by ^{1}H NMR spectroscopic experiments (Fig. 3a). Upon addition of 1.0 equiv. of WBT, all of the protons of spermine showed remarkable upfield shifts ($\Delta\delta = -0.65$, -0.85, -0.98, -0.44 and -0.85 ppm for H_1, H_3, H_4, H_2 and H_5, respectively). These protons also displayed significant broadening effects. These results suggested that protons of spermine were encapsulated by WBT's cavity. 2D NOESY NMR of an aqueous solution of WBT (5 mmol/L) and spermine (5 mmol/L) showed distinct NOE correlation signals (such as H_5 of spermine and H_d, H_e, H_f of WBT), which further confirmed the formation of an inclusion complex (Fig. S15 in Supporting information). It was found that in the presence of approximately 1.0 equiv. WBT, proton signals from other biogenic amines also show upfield shifts, but the NMR changes are smaller than that of spermine (Figs. S16-S22 in Supporting information). To determine the binding affinity of WBT towards different types of biogenic amines, UV–vis titration experiments were performed in sodium phosphate buffer (pH 7.4) (Fig. 3b). Job plot showed the binding stoichiometry of the water-soluble host WBT with these biogenic amine guests were 1:1 (Fig. S23 in Supporting information). The association constant (K_a) determined *via* nonlinear fitting for spermine is up to 2.9×10^5 L/mol which is higher than other aliphatic amines (Fig. 3c, Table 1 and Figs. S24-S27 in Supporting information). For aromatic and heterocyclic amines, their K_a values are in the order of magnitude of 10^2–10^3 L/mol (Figs. S28-S30 in Supporting information). Obviously, aliphatic spermine exhibited stronger binding affinities than others. The highest binding affinity of spermine may be due to its polycationic nature, which contributes to tighter recognition by multiple electrostatic interactions between carboxylate and amino groups. Combined with AIE effect of the water-soluble macrocycle, it should be feasible to achieve selective detection of spermine by means of these different affinities.

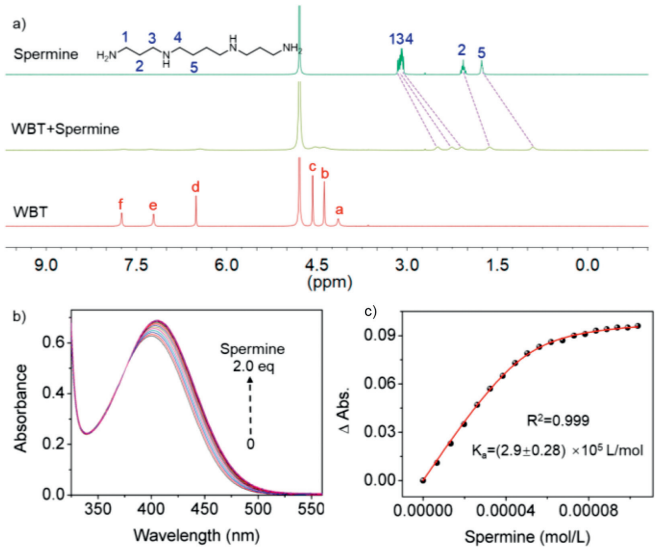

Fig. 3. (a) ^{1}H NMR spectra (400 MHz, D_2O, 0.5 mmol/L) of spermine (top), WBT in the presence of spermine (middle) and WBT (bottom). (b) UV–vis spectra of WBT (50 μmol/L) in sodium phosphate buffer (pH 7.4) recorded in the presence of different concentrations of spermine at 298 K. (c) Nonlinear least-squares fitting at 415 nm to calculate the K_a value.

Table 1
Association constants (K_a) of WBT with biogenic amines in 20 mmol/L sodium phosphate buffer (pH 7.4) at 298 K.

Biogenic amines	K_a (L/mol)
Spermine	$(2.9 \pm 0.28) \times 10^5$
Spermidine	$(3.5 \pm 0.29) \times 10^4$
Agmatine	$(9.8 \pm 0.50) \times 10^3$
Cadaverine	$(2.4 \pm 0.10) \times 10^3$
Octopamine	$(3.8 \pm 0.18) \times 10^3$
Dopamine	$(1.2 \pm 0.10) \times 10^3$
Histamine	$(8.4 \pm 0.35) \times 10^2$
Putreanine	$(1.4 \pm 0.10) \times 10^3$

The fluorescence response of WBT to spermine was then examined. As seen in Fig. 4a, the fluorescence intensity of WBT increased after addition of spermine, which might be due to binding-induced aggregation. The emission intensity-concentration correlation curve showed (Fig. 4b) that the fluorescence intensity at 625 nm of WBT was linearly increased with spermine concentration below 118 μmol/L. When the analyte concentration went above this range, the emission intensity was further increased, but the change was beginning to slow down. In contrast, other biogenic amines did not induce a major change in fluorescence intensity (Figs. S31-S37 in Supporting information), which indicated selective responses of WBT toward spermine (Fig. 4c). Therefore, WBT could be used for the selective detection of spermine towards

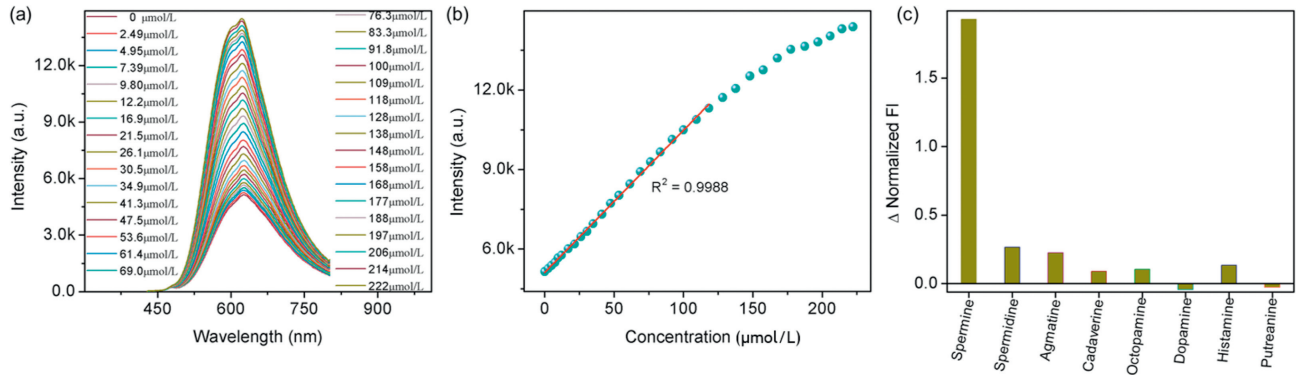

Fig. 4. (a) The fluorescence intensity response of WBT (50 μmol/L) to spermine at varied concentrations. (b) Fluorescence intensity change of WBT at 625 nm in the presence of different concentration of spermine. Solvent: 20 mmol/L sodium phosphate buffer (pH 7.4). Excitation wavelength: 410 nm, em/ex slits = 5 nm. (c) Change in fluorescence intensity of WBT with 4 equiv. of biological amines.

a variety of biological amines. The detection limit for spermine was calculated to be 0.54 μmol/L (Fig. S38 in Supporting information), which was low enough to detect pathological situations (*e.g.*, urinary spermine concentration of cancer patients range of 1–10 μmol/L) [42,43].

In summary, we have synthesized a novel anionic water-soluble macrocycle with AIE effect (WBT). WBT was constructed on the basis of benzothiadiazole rather than typical AIE luminogens tetraphenylethene. It displayed a good aqueous solubility, AIE property and concentration-dependent fluorescence enhancement phenomenon. Compared to other biogenic amines, it exhibited stronger binding affinities towards spermine with association constants of 2.9×10^5 L/mol in aqueous media. The different binding affinities made the water-soluble macrocycle to achieve selective detection of spermine. Developing new water-soluble macrocycle with multifunction provided a simple strategy for the detection of biomolecules.

Declaration of competing interest

The authors declare that they have no known competing financial interests or personal relationships that could have appeared to influence the work reported in this paper.

Acknowledgments

The authors are grateful to the Natural Science Foundation of Zhejiang Province (Nos. LR24B020003 and LQ24B020003) and the National Natural Science Foundation of China (No. 21921003) for financial support.

Supplementary materials

Supplementary material associated with this article can be found, in the online version, at doi:10.1016/j.cclet.2024.109791.

References

[1] I. Roy, A.H.G. David, P.J. Das, D.J. Pe, J.F. Stoddart, Chem. Soc. Rev. 51 (2022) 5557–5605.
[2] H.T. Feng, Y.X. Yuan, J.B. Xiong, Y.S. Zheng, B.Z. Tang, Chem. Soc. Rev. 47 (2018) 7452–7476.
[3] T.L. Mako, J.M. Racicot, M. Levine, Chem. Rev. 119 (2019) 322–477.
[4] L. Bian, Y. Liang, Z. Liu, A.C.S. Appl, Nano Mater. 5 (2022) 13940–13958.
[5] T. Li, X. Zhu, G. Ouyang, M. Liu, Mater. Chem. Front. 7 (2023) 3879–3903.
[6] M. Hasegawa, Y. Nojima, Y. Mazaki, ChemPhotoChem 5 (2021) 1042–1058.
[7] S. Zhong, L. Zhu, S. Wu, Y. Li, M. Lin, Chin. Chem. Lett. 34 (2023) 108124.
[8] L. Zhu, W. Zeng, M. Li, M. Lin, Chin. Chem. Lett. 33 (2022) 229–233.
[9] D. Li, F. Lu, J. Wang, et al., J. Am. Chem. Soc. 140 (2018) 1916–1923.
[10] X.N. Han, Q.S. Zong, Y. Han, C.F. Chen, CCS Chem. 4 (2022) 318–330.
[11] S.N. Lei, H. Xiao, Y. Zeng, et al., Angew. Chem. Int. Ed. 59 (2020) 10059–10065.
[12] C. Tu, W. Wu, W. Liang, et al., Angew. Chem. Int. Ed. 61 (2022) e202203541.
[13] P. Chen, F. Jakle, J. Am. Chem. Soc. 133 (2011) 20142–20145.
[14] S. Li, Z.Y. Zhang, H. Zhang, et al., Org. Chem. Front. 9 (2022) 4394–4400.
[15] S. Song, H.F. Zheng, H.T. Feng, Y.S. Zheng, Chem. Commun. 50 (2014) 15212–15215.
[16] Y. Sun, L. Jiang, L. Liu, et al., Adv. Optical. Mater. 11 (2023) 2300326.
[17] M. Lin, L. Bian, Q. Chen, et al., Angew. Chem. Int. Ed. 62 (2023) e202303035.
[18] L. Mao, F. Li, L. Huang, X. Qu, et al., Org. Lett. 25 (2023) 5597–5601.
[19] S. Jiang, J. Yang, L. Ling, S. Wang, D. Ma, Anal. Chem. 94 (2022) 5634–5641.
[20] H. Nian, L. Cheng, L. Wang, et al., Angew. Chem. Int. Ed. 133 (2021) 15482.
[21] Y. Liu, H. Wang, L. Shangguan, et al., J. Am. Chem. Soc. 143 (2021) 3081.
[22] T.X. Zhang, Z.Z. Zhang, Y.X. Yue, et al., Adv. Mater. 32 (2020) 1908435.
[23] T. Türel, S. Valiyaveettil, ChemPlusChem 85 (2020) 1430.
[24] M. Sapotta, A. Hofmann, D. Bialas, F. Würthner, Angew. Chem. Int. Ed. 58 (2019) 3516.
[25] G. Li, L. Zhao, P. Yang, et al., Anal. Chem. 88 (2016) 10751–10756.
[26] H. Yao, Q. Zhou, J. Wang, et al., Spectrochim. Acta Mol. Biomol. Spectrosc. 221 (2019) 117215.
[27] L. Zhang, Y. Xu, W. Wei, Chem. Commun. 59 (2023) 13562–13570.
[28] F. Würthner, Angew. Chem. Int. Ed. 59 (2020) 14192–14196.
[29] Y. Wang, J. Nie, W. Fang, et al., Chem. Rev. 120 (2020) 4534–4577.
[30] Y.F. Wang, T. Zhang, X.J. Liang, Small 12 (2016) 6451–6477.
[31] L. Mao, Y. Liu, S. Yang, Y. Li, X. Zhang, Y. Wei, Dyes Pigm. 162 (2019) 611–623.
[32] M.H. Chua, K.W. Shah, H. Zhou, J. Xu, Molecules 24 (2019) 2711.
[33] X.M. Sun, J. Liu, Z.H. Li, et al., Chin. Chem. Lett. 34 (2023) 107792.
[34] Y. Liu, Z. Guo, Y. Guo, et al., Chin. Chem. Lett. 34 (2023) 108531.
[35] X.Y. Lou, G. Zhang, N. Song, Y.W. Yang, Biomaterials 286 (2022) 121595.
[36] J.H. Wang, H.T. Feng, J. Luo, Y.S. Zheng, J. Org. Chem. 79 (2014) 5746–5751.
[37] H. Duan, F. Cao, M. Zhang, M. Gao, L. Cao, Chin. Chem. Lett. 33 (2022) 2459–2463.
[38] X. Tian, M. Zuo, P. Niu, et al., ACS Appl. Mater. Interfaces 13 (2021) 37466–37474.
[39] S. Li, K. Liu, X.C. Feng, et al., Nat. Commun. 13 (2022) 2850.
[40] B. Lu, L. Wang, X. Ran, H. Tang, D. Cao, Biosensors 12 (2022) 633.
[41] M. Barros, S. Ceballos, P. Arroyo, et al., Chemosensors 10 (2021) 8.
[42] J.A. Byun, M.H. Choi, M.H. Moon, B. Kong, B.C. Chung, Cancer Lett. 273 (2009) 300–304.
[43] J. Tu, S. Sun, Y. Xu, Chem. Commun. 52 (2016) 1040–1043.